

Self-Healing Behavior of Oxide Layer in Liquid Metal^{*)}

Atsushi KAWARAI and Masatoshi KONDO¹⁾

*Tokyo Institute of Technology, School of Engineering, Department of Mechanical Engineering,
Ookayama, Meguro-ku, Tokyo 152-8550, Japan*

¹⁾*Tokyo Institute of Technology, Institute of Innovative Research, Laboratory for Zero-Carbon Energy,
Ookayama, Meguro-ku, Tokyo 152-8550, Japan*

(Received 9 January 2022 / Accepted 15 March 2022)

The dynamic behaviors of oxide layer formation, growth and self-healing in liquid metal lead (Pb) were studied by on-line monitoring with electrochemical impedance spectroscopy (EIS). The metal rod made of zirconium (Zr) was immersed to liquid Pb at 773 K as the working electrode of EIS. The capacitance semicircle due to the oxide layer formation on the rod surface was detected by EIS after the immersion for 45 hr. The increase of impedance due to the growth of the oxide layer in liquid Pb was continuously detected. The rod was taken out from liquid Pb after the immersion for 150 hr, and the oxide layer formed on the rod was partially exfoliated using lathe to simulate the damage of the oxide layer. The rod was immersed again to liquid Pb for 200 hr. The capacitance semicircle due to the self-healing of the oxide layer was recognized after the immersion for 126 hr. The self-healing of the artificially damaged area on the oxide layer was recognized by the microscopic analysis.

© 2022 The Japan Society of Plasma Science and Nuclear Fusion Research

Keywords: electrochemical impedance spectroscopy, liquid metal, oxide layer, self-healing

DOI: 10.1585/pfr.17.2405059

1. Introduction

Liquid metal lithium lead (LiPb) is tritium breeder of fusion reactors [1–3]. Liquid metal lead (Pb) is a promising neutron multiplier [4]. The development of functional layers such as a tritium permeation barrier (TPB), an electrical insulation layer and an anti-corrosion layer is essential for the design of the liquid metal based in-vessel components.

Zirconium (Zr) can form the layer of zirconium oxide (i.e. ZrO_2) on its surface, when the oxygen potential in liquid metal is sufficiently high. This layer is chemically compatible with liquid metals Pb and LiPb [5]. The layer also has a large electrical resistivity which is preferable feature as an electrical insulation layer [6]. The layer also has an excellent performance as TPB [7]. The layer of Zr metal can be laminated on structural materials by plasma activated sintering, and the Zr layer can form Zr oxide layer on its surface.

The self-healing function of the ZrO_2 layer during the operation of reactor components can improve their reliability. The layer can be self-healed by the oxidation with oxygen dissolved in liquid metals even when the layer was partially exfoliated [8]. However, the self-healing behavior of the oxide layer in liquid metals has rarely been studied so far. Electrochemical impedance spectroscopy (EIS) is able to obtain the electrical characteristics of oxide layers formed on the metal surface in liquid metals Pb and Pb-

Bi [9–11]. The dynamic behaviors of oxide layer formation, growth and self-healing in liquid metal can be in-situ monitored by the EIS technique.

The purpose of the present study is to make clear the self-healing behaviors of oxide layer in liquid metal Pb. The oxide layer formed on the surface of Zr rod electrode in liquid Pb was artificially damaged. The specimen with damaged oxide layer was then exposed to the liquid metal for its self-healing, and the dynamic behavior was in-situ monitored by EIS. The microscopic observation and analysis on the self-healed area of the oxide layer were also performed.

2. Experimental Conditions

2.1 Experimental apparatus

Figure 1 shows the experimental apparatus. The liquid temperature was monitored by the thermocouple directly immersed into liquid Pb. The diameter of the rod-shaped Zr specimen was 6 mm. The rod-shaped Zr specimen was immersed to liquid Pb as the working electrode of EIS. The rod made of 316L was immersed as the counter electrode. The volume of liquid Pb was approximately 36 cc. The cover gas inside the vessel was high-purity Ar and the pressure was 1 atm.

The solid electrolyte oxygen sensor was installed in liquid Pb [12] to monitor the oxygen concentration. The sensor cell was made of yttria stabilized zirconia. The powder of Fe/Fe_3O_4 was used as reference electrode [13]. The electrochemical system of the sensor is expressed as follows:

Corresponding author's e-mail: kondo.m.ai@m.titech.ac.jp

^{*)} This article is based on the presentation at the 30th International Toki Conference on Plasma and Fusion Research (ITC30).

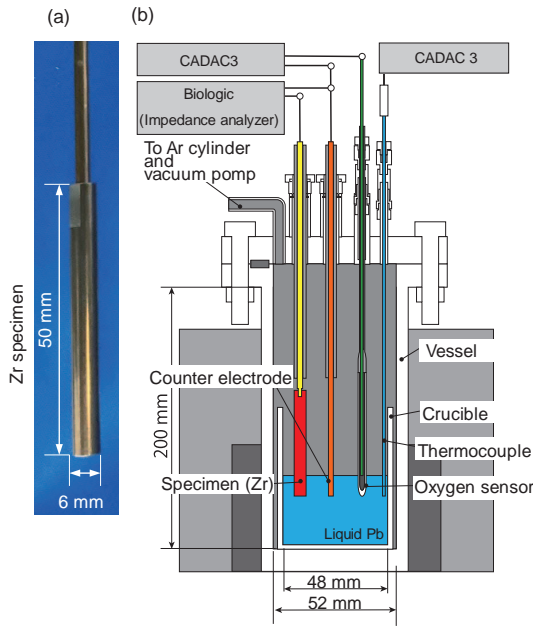


Fig. 1 Experimental apparatus (a) Zr rod and (b) liquid metal test vessel with EIS system.

$$[\text{Fe} - \text{Fe}_3\text{O}_4]/[\text{Y}_2\text{O}_3 + \text{ZrO}_2]/[\text{Pb}]. \quad (1)$$

The electromotive force induced by the difference of oxygen potential in between the reference electrode and liquid Pb is expressed by the Nernst equation as follows:

$$E = \frac{RT}{4F} \ln \frac{P_{\text{reference}}}{P_{\text{Liquid Pb}}}, \quad (2)$$

where $P_{\text{reference}}$ and $P_{\text{Liquid Pb}}$ are the equilibrium oxygen partial pressures in the reference electrode and liquid Pb, respectively. T [K] is the temperature of liquid Pb, R [$\text{J K}^{-1} \text{mol}^{-1}$] is gas constant and F [C/mol] is Faraday constant. The equilibrium oxygen partial pressures are expressed as follows:

$$P_{\text{reference}} = \exp\left(\frac{\Delta G_{\text{Fe}_3\text{O}_4}^0}{2RT}\right), \quad (3)$$

$$P_{\text{Liquid Pb}} = \left(\frac{c}{c_s}\right)^2 \exp\left(\frac{2\Delta G_{\text{PbO}}^0}{RT}\right), \quad (4)$$

where c [wt%] is the oxygen concentration in liquid Pb, c_s [wt%] is the oxygen solubility in liquid Pb and ΔG^0 [$\text{J}^{-1} \text{mol}$] is standard free energy of formation of each substance. The oxygen solubility c_s [wt%] in liquid Pb is expressed as follows [14]:

$$\log c_s = 3.23 - \frac{5043}{T}. \quad (5)$$

The oxygen concentration in liquid Pb was not actively controlled in the present study.

2.2 Experimental conditions

Liquid Pb is candidate neutron multiplier [4]. ZrO_2 is chemically compatible both with liquid Pb [15] and LiPb

[16]. The oxygen potential of liquid Pb is higher than that of liquid LiPb. The oxidation behavior of Zr metal in liquid Pb is simpler than that in liquid LiPb, since the Li component does not contribute to the oxidation behavior.

The experimental procedures were summarized in Fig. 2. The temperature of liquid Pb was kept at 773 K during the experiment. Zr-rod specimen was immersed to liquid Pb for 150 hr in the first immersion test. The immersion depth was 10 mm as shown in Fig. 2 (a). The oxide layer was formed on the immersed area due to the oxidation in the liquid Pb (Fig. 2 (b)). This behavior was monitored by EIS.

The Zr rod was taken out from liquid Pb after the first immersion test. The oxide layer formed on the Zr rod was partially removed by lathe to simulate the local damage of the oxide layer as shown in Fig. 2 (c). The area with this artificial exfoliation is referred to as exfoliated area in this paper. The rest is referred to as non-exfoliated area. The exfoliated area had a width of 1 mm and a depth of $8 \mu\text{m}$. The exfoliated area revealed a metallic luster.

The Zr rod which had the oxide layer artificially damaged was immersed again to liquid Pb. The immersion depth was 8 mm so that the area where oxide layer was not formed in the first immersion did not contact with liquid Pb. The self-healing of the oxide layer was induced by the formation of new oxide layer on the exfoliated area, where was directly exposed to liquid metal (Fig. 2 (d)).

The EIS was continuously conducted to detect the formation, growth and self-healing of the oxide layer every 5 minutes in the first and second immersion tests. The amplitude of AC voltage was 500 mV, and the frequency of the AC voltage was in the range between 100 mHz to 1 MHz. The EIS was carried out with Bio-Logic SP-150 (Bio-Logic Science Instruments).

The output of the solid electrolyte oxygen sensor indicated that the oxygen concentration in liquid Pb was kept between $1.06 \times 10^{-4} \sim 4.75 \times 10^{-4}$ wt% in the first immersion test, and $1.42 \times 10^{-4} \sim 2.24 \times 10^{-4}$ wt% in the second immersion test. These oxygen concentrations indicated that oxygen potential in liquid Pb was higher than that for the formation of ZrO_2 .

Three-dimensional geometry around the exfoliated area on the Zr rod was analyzed by 3D laser scanning microscope (LSM) before and after the self-healing of oxide layer. The cross-sectional characterization around the self-healed area was also performed by scanning electron microscope (SEM) with energy dispersive X-ray spectroscopy (EDX) to clarify the thickness and chemical compositions of the layer after the second immersion test.

3. Results and Discussions

3.1 Formation and growth of oxide layer in liquid Pb

The formation of homogenous oxide layer is electrically expressed by RC parallel circuit as shown in Fig. 3,

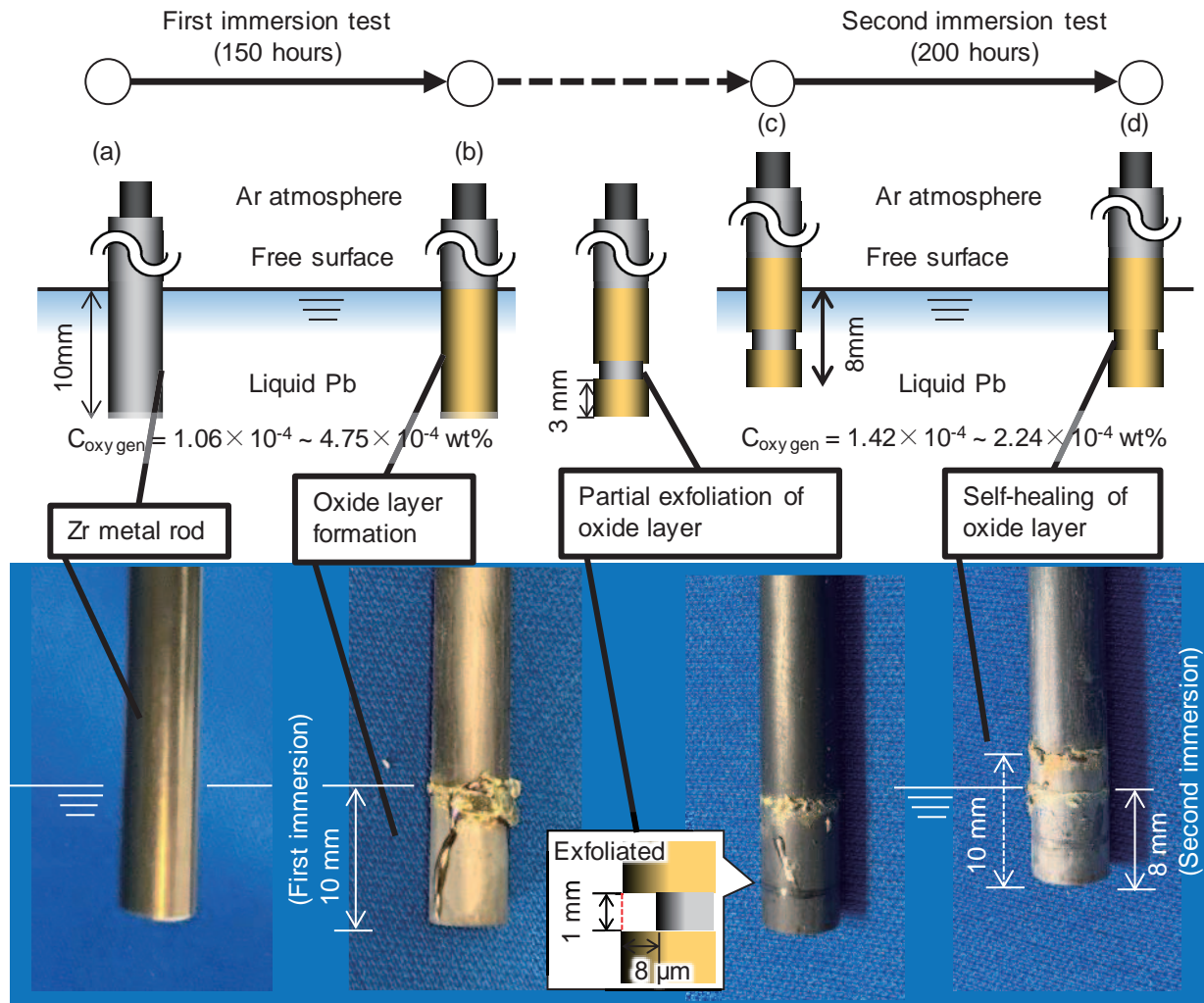


Fig. 2 Experiment procedures: (a) Initial condition of Zr rod, (b) Oxide layer formed on immersed area in first immersion test, (c) Partial exfoliation of oxide layer by lathe and (d) Self-healed oxide layer in second immersion test.

and the Nyquist plot of the frequency response draws so-called capacitance semicircle according to the electrical circuit [17]. The capacitance semicircle was obtained by EIS after the immersion for 45 hr as shown in Fig. 4, which indicated the formation of oxide layer. EIS response could not be obtained due to small electrical impedance of the interface between the Zr rod and liquid Pb in the initial 45 hr of the first immersion test.

The diameter of the capacitance semicircle expanded with time as shown in Fig. 5. This behavior indicated the increase of impedance according to the growth of oxide layer and the increase of layer thickness in liquid Pb [18]. The initial metallic luster of the Zr rod was lost in the immersed area due to the oxide layer formation as shown in Fig. 2 (b). The thickness of the oxide layer t [μm] can be derived as follows:

$$t = \frac{AR}{\rho}, \tag{6}$$

where A [m^2] is the immersed area of the Zr rod in liquid Pb, R [Ω] is the electrical resistance of the oxide layer and

ρ [Ωm] is the electrical resistivity of the oxide layer. The electrical resistance of the oxide layer formed and grew by the immersion for 200 hr was 155 M Ω . The layer thickness was estimated as 2.67 μm , when the electrical resistivity of ZrO_2 at 773 K was given as 1.26×10^{10} Ωm in the literature [18]. This layer thickness was reasonable as explained in the latter chapter.

3.2 Self-healing behaviors of oxide layer in liquid Pb

The on-line EIS analysis was conducted in the same way with the first immersion test. The capacitance semicircle was not obtained in the initial stage of the second immersion test due to the electrical conduction through the exfoliated area on the specimen rod. The capacitance semicircle was recognized after the exposure for 126 hr in the second immersion test as shown in Fig. 6. The longer time was needed to obtain the capacitance semicircle than that in the first immersion test. The capacitance semicircle obtained after the immersion for 196 hr was also shown in

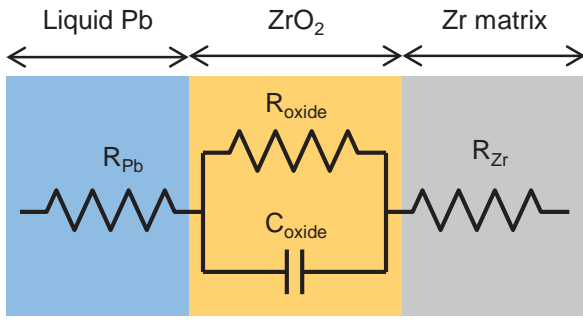


Fig. 3 Equivalent RC circuit of oxide layer formed on Zr rod in liquid Pb.

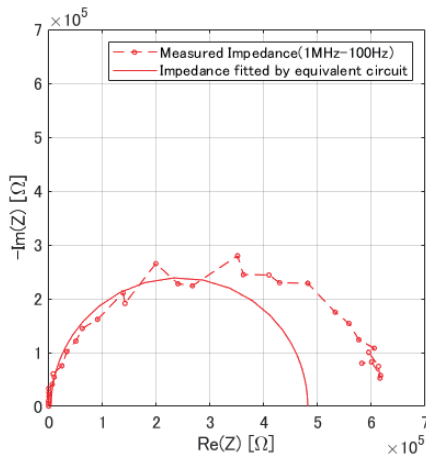


Fig. 4 Capacitance semicircle obtained after 45 hr at first immersion.

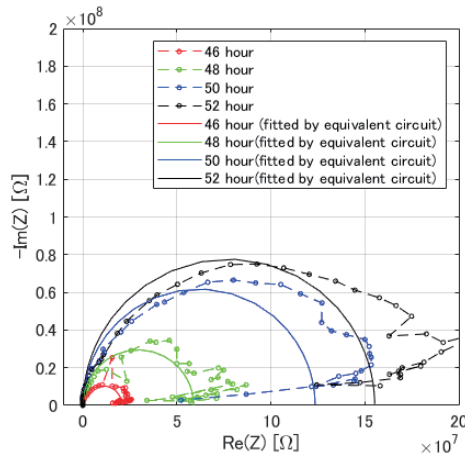


Fig. 5 Capacitance semicircles obtained in experiment for 46 hr to 52 hr in first immersion experiment.

Fig. 6. The capacitance semicircle did not grow significantly even after the additional immersion for 70 hr. The growth ratio of the oxide layer was smaller than that recognized in the first immersion test. The exfoliated area could have larger surface roughness than original surface since it was partially machined by lathe. The formation

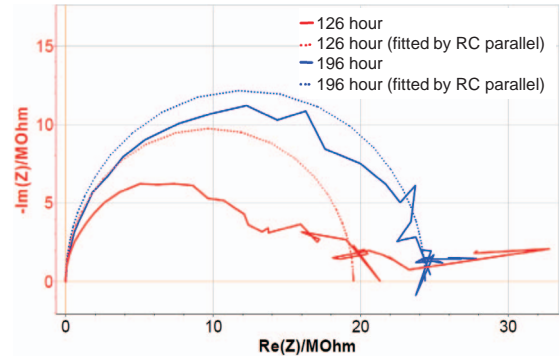


Fig. 6 Capacitance semicircles obtained after immersion to liquid Pb for 126 and 196 hr in second immersion test.

and growth of the uniform oxide layer was inhibited on the rough surface. This capacitance semicircle could represent the impedance of thinner oxide layer newly formed on the exfoliated area since the electrical resistance was much less than that of non-exfoliated area.

The depressed capacitance semicircle obtained in the measurement after the immersion for 126 hr can be explained based on the parallel circuit with resistance and constant phase element (CPE) [19]. Impedance of RC parallel circuit and R-CPE parallel circuit is expressed as follows:

$$Z = \frac{R}{1 + j\omega CR}, \tag{7}$$

$$Z = \frac{R}{1 + (j\omega)^p YR}, \tag{8}$$

where Z [Ω] is the impedance, R [Ω] is the resistance, ω [rad s^{-1}] is the angular frequency, C [F] is the capacitance, j is imaginary unit, p is the CPE exponent and Y is the CPE constant. The CPE exponent p takes the value between 0 and 1, and this value closes to 1 when the electrode conditions are homogenous [20]. The electrode conditions are determined by the oxide layer characteristics in the present study. Eq. (8) can draw depressed semi-circle on Nyquist plot when the CPE exponent p is small. The capacitance semicircle revealed higher CPE exponent after the immersion for 196 hr as shown in Fig. 6, though the semicircle obtained after 126 hr revealed the depressed shape. This behavior indicated that the oxide layer on the Zr rod became more homogeneous.

The metallic luster of the exfoliated area on the specimen rod was not recognized after the second immersion test for 200 hr as shown in Fig. 2 (d). Figures 7 (a) and (b) shows the three-dimensional geometry of the exfoliated area before and after the second immersion test, respectively. The surface profiles before and after the second immersion test shown in Figs. 7 (a) and (b) were obtained by the average. The averaged depth of the exfoliated area was approximately $2 \mu\text{m}$ after the second immersion test, though that before the second immersion test was approximately $8 \mu\text{m}$ as shown in Fig. 7 (c). The depth was reduced

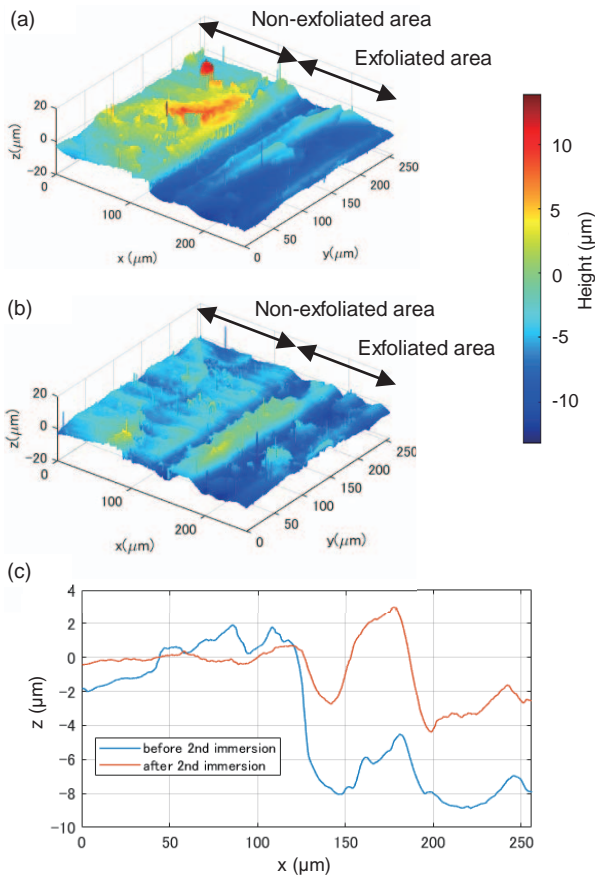


Fig. 7 (a) 3D surface geometry by LSM after 150-hour immersion to liquid Pb and partial exfoliation of oxide layer, (b) 3D surface geometry by LSM after self-healing of oxide layer in liquid Pb and (c) Surface profiles along x direction by average on all areas shown in Figs. 7 (a) and (b).

because of the formation and growth of the oxide layer and oxygen diffusion zone on the exfoliated area.

Figure 8 (a) shows the SEM cross-sectional image around the self-healed area. Figure 8 (b) shows the results of EDX analysis along lines (i) and (ii) on the oxide layer in Fig. 8 (a). The ZrO_2 layer which had a thickness of approximately $5 \mu m$ was detected by EDX in non-exfoliated area as shown in Fig. 8 (b). The thickness after the first immersion test for 150 hr was estimated as $2.67 \mu m$ from the impedance information of EIS and Eq. (6), though the layer thickness was not microscopically measured. This thickness was reasonable when the test duration was taken into account. Fig. 8 (b) indicates the formation of oxygen diffusion zone where the atomic ratio of Zr and O is 1:1 beneath the oxide layer. This oxygen diffusion zone had a thickness of $6 \mu m$. The oxygen diffusion zone was electrically conductive and was not detected by EIS.

The oxide layer which had a thickness of approximately $1-2 \mu m$ was detected on the exfoliated area as shown in Fig. 8 (b). Therefore, the thickness of the oxide layer formed on the exfoliated area was thinner than that on non-exfoliated area. The exfoliated area also had an oxy-

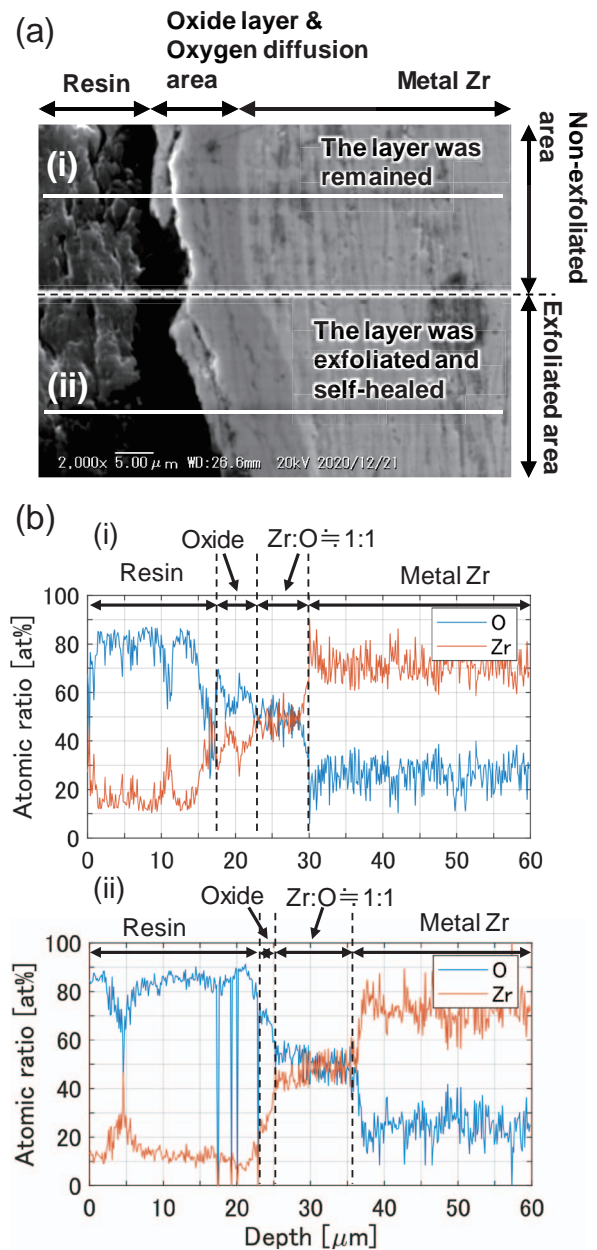


Fig. 8 (a) Cross-sectional SEM image around self-healed area of Zr rod in liquid Pb and (b) EDX analysis on chemical compositions of oxide layer and oxygen diffusion zone along line (i) and line (ii).

gen diffusion zone, and the thickness was approximately $10 \mu m$ which was thicker than that on non-exfoliated area. The formation of oxygen diffusion zone in the Zr metal matrix might be promoted when the surface was not protected by ZrO_2 layer. The formation of ZrO_2 layer needed longer time than the formation of the oxygen diffusion zone. The thickness of the oxygen diffusion zone was reduced by the immersion for longer duration, though the oxide layer was formed on the oxygen diffusion zone. These results indicated the the oxide layer might be formed in the oxygen diffusion zone.

4. Conclusions

Major conclusions are follows:

1. The Zr metal rod was oxidized in liquid Pb at 773 K. Both the oxide layer and the oxygen diffusion zone were formed on the surface of the Zr rod.
2. The impedance of Zr oxide layer formed on the Zr rod in liquid Pb were in-situ measured by EIS. The EIS results indicated the expansion of a capacitance semi-circle according to the growth of the oxide layer.
3. The Zr rod immersed in liquid Pb for 150 hr was taken out from the melt. The Zr oxide layer formed on the rod was partially exfoliated by lathe. The rod was then immersed again to liquid Pb. The EIS output indicated the self-healing of the oxide layer according to the formation of new oxide layer on the exfoliated area.

Acknowledgement

Authors would acknowledge Dr. Tada of Open Facility Center, Materials Analysis Division, Tokyo Institute of Technology, for his technical assistance on SEM/EDX analysis, and Ms. Mochinaga of Tokyo Institute of Technology for her technical assistance on 3D laser scanning microscope observation. This study was partially supported by JSPS KAKENHI Grant-in-Aid for Scientific Research (B) 21H01060.

- [1] T. Muroga and B.A. Pint, *Fusion Eng. Des.* **85**, 1301 (2010).
- [2] A. Suzuki, T. Chikada and T. Tanaka, *J. Plasma Fusion Res.* **89**, 349 (2013).
- [3] M. Kondo, M. Takahashi, T. Tanaka, V. Tsisar and T. Muroga, *Fusion Eng. Des.* **87**, 1777 (2012).
- [4] F.A. Hernández and P. Pereslavtsev, *Fusion Eng. Des.* **137**, 243 (2018).
- [5] T. Chikada, A. Suzuki, T. Terai, T. Muroga and F. Koch, *Fusion Eng. Des.* **88**, 6-8, 640 (2013).
- [6] T. Tanaka and T. Norimatsu, *J. Plasma Fusion Res.* **92**, 2, 112 (2016).
- [7] H. Nakamura, K. Isobe, M. Nakamichi and T. Yamanishi, *Fusion Eng. Des.* **85**, 1531 (2010).
- [8] Z. Yao, A. Suzuki, T. Muroga and T. Nagasaka, *Fusion Eng. Des.* **81**, 2887 (2006).
- [9] M. Kondo, N. Suzuki, Y. Nakajima T. Tanaka and T. Muroga, *Fusion Eng. Des.* **89**, 1201 (2014).
- [10] J.F. Stubbins, A.M. Bolind and X. Chen, *J. Nucl. Mater.* **377**, 1, 243 (2008).
- [11] X. Chen, R. Haasch and J.F. Stubbins, *J. Nucl. Mater.* **431**, 1-3, 125 (2012).
- [12] M. Kondo, M. Takahashi, K. Miura and T. Onizawa, *J. Nucl. Mater.* **357**, 1-3, 97 (2006).
- [13] P.M. Adhi, M. Kondo and M. Takahashi, *Sens. Actuators B Chem.* **241**, 1261 (2017).
- [14] Nuclear Energy Agency, *Handbook on Lead-bismuth Eutectic Alloy and Lead Properties, Materials Compatibility, Thermal-hydraulics and Technologies* (2015) p. 156.
- [15] M. Kondo, P. Adhi, M. Takahashi, N. Suzuki, Y. Matsumura, T. Tanaka, Y. Hishinuma, A. Sagara and T. Muroga, *Transactions of the JSME* **83**, 847, 16-00412 (2017).
- [16] S. Miura, K. Nakamura, E. Akahoshi, S. Kano, J. Yagi, Y. Hishinuma, T. Tanaka and T. Chikada, *Fusion Eng. Des.* **170**, 112536 (2021).
- [17] H. Katayama, *J. Japan Inst. Met. Mater.* **78**, 11, 419 (2014).
- [18] N. Suzuki, R. Sasaki, Y. Matsumura and M. Kondo, *J. Japan Inst. Met. Mater.* **80**, 4, 284 (2016).
- [19] T. Pajikossy, *J. Electroanal. Chem.* **364**, 111 (1994).
- [20] P. Zoltowski, *J. Electroanal. Chem.* **443**, 149 (1998).